What Makes for a Good Catalytic Cycle? A Theoretical Study of the Role of an Anionic Palladium(0) Complex in the Cross-Coupling of an Aryl Halide with an Anionic Nucleophile†

Sebastian Kozuch, Christian Amatore,§ Anny Jutand,§ and Sason Shaik*,‡

Department of Organic Chemistry and the Lise Meitner-Minerva Center for Computational Quantum Chemistry, The Hebrew University of Jerusalem, Givat Ram Campus, Jerusalem 91904, Israel, and Ecole Normale Supérieure, Département de Chimie, UMR CNRS-ENS-UPMC 8640, 24 Rue Lhomond, F-75231 Paris Cedex, France

Received March 6, 2005

The cross-coupling reaction Ar−X + Nu^- → Ar−Nu + X^-, catalyzed by Pd(0) complexes, was studied theoretically by means of DFT calculations; Ph−Cl was used as a substrate and HS^- as the nucleophile. The studied catalysts are the pristine Pd(0) complexes $Pd^0(PR_3)_2$ (**1**$_R$; R = H, vinyl, Ph), the corresponding anionic complexes $Pd^0(PR_3)_2Cl^-$ (**1**$_{R,Cl}$), proposed by two of us (C.A. and A.J.), and the chelated complexes with diphosphine ligands $PH_2(CH_2)_nPH_2$ (**2**$_{H,n}$; n = 2−6). The full catalytic cycles were studied for **1**$_H$, **1**$_{H,Cl}$, **2**$_{H,3}$, and **2**$_{H,6}$. The efficiency of a catalytic cycle under turnover conditions is determined by the energetic span, the energy difference between the summit and trough of the cycle; *the smaller the energy span, the higher the turnover frequency of the cycle.* In this sense, the best Pd(0) catalyst was found to be the anionic **1**$_{H,Cl}$ species. The DFT analysis shows that the anionic catalyst so formed is superior to the pristine species, since it "flattens" the energy landscape of the catalytic cycle by stabilizing the transition state for oxidative addition, the summit of the cycle, and at the same time "destabilizing" the nucleophilic addition product, the deepest point of the cycle. This is precisely the role deduced initially from experimental evidence. Thus, during substrate activation, the Cl^- ion keeps a small P−Pd−P angle, which is a prerequisite for a low activation barrier to oxidative addition. During nucleophilic substitution, the Cl^- additive is displaced by the nucleophile, and hence the stabilizing advantage is lost, thereby raising the substitution product complex relative to the onset of the reactants. After product release, Cl^- returns to regenerate the anionic catalyst, $Pd^0(PR_3)_2Cl^-$, which in turn binds the substrate and prevents its diffusive escape, thereby ensuring an efficient restart of the cycle.

Introduction

Palladium is being rediscovered as a versatile catalyst and as the generator of a variety of organic molecules. Some of its reactions, such as the Heck, Tsuji−Trost, Suzuki, Sonogashira, and cross-Ccoupling reactions, are considered as fundamental building blocks in organic chemistry laboratories[1] and chemical industry.[2] The ability of the catalyst to cleave C−X bonds (X = halide, AcO, etc.), the starting point for the majority of the catalytic cycles of these reactions, is a key step that affects the efficiency of these cycles. In this step, a Pd(0) complex undergoes oxidative addition to form a Pd(II) complex, which then proceeds in a variety of ways, depending on the transformation at hand. Using as an example the cross-coupling reaction with a powerful anionic nucleophile, the consensus ("textbook") mechanism is based on the "pristine" linear Pd^0L_2 complex, which initiates the cycle, as shown in Scheme 1a. In the early 1990s and afterward, a new mechanism was proposed by two of us (A.J. and C.A.),[3−8] on the basis of the observation that the catalytic action of the Pd^0L_2

* To whom correspondence should be addressed. E-mail: sason@yfaat.ch.huji.ac.il. Fax: +972−2−6584680.

† Dedicated to M. A. Robb on the occasion of his forthcoming 60th birthday.

‡ The Hebrew University of Jerusalem.

§ UMR CNTS-ENS-UPMC 8640.

(1) For a small selection of experimental papers, see: (a) Tykwinski, R. R. *Angew. Chem., Int. Ed.* **2003**, *42*, 1566−1568; *Angew. Chem.* **2003**, *115*, 1604−1606. (b) von Schenck, H.; Akerman, B.; Svensson, M. *J. Am. Chem. Soc.* **2003**, *125*, 3503−3508. (c) Culkin. D. A.; Hartwig. J. F. *Acc. Chem. Res.* **2003**, *36*, 234−245. (d) Bhattacharyya, S.; Weakley, T. J. R.; Chaudhury, M. *Inorg. Chem.* **1999**, *38*, 5453−5456. (e) Hassan, J.; Sevignon, M.; Gozzi, C.; Schulz, E.; Lemaire, M. *Chem. Rev.* **2002**, *102*, 1359−1469. (f) Kim, Y. M.; Yu, S. *J. Am. Chem. Soc.* **2003**, *125*, 1696−1697. (g) Negishi, E. *Acc. Chem. Res.* **1982**, *15*, 340−348. (h) Negishi, E. *J. Am. Chem. Soc.* **1987**, *109*, 2393−2401. (i) Beletskaya, I. P.; Cheprakov, A. V. *Chem. Rev.* **2000**, *100*, 3009−3066. (j) Littke, A. F.; Fu, G. C. *Angew. Chem., Int. Ed.* **2002**, *41*, 4176−4211; *Angew. Chem.* **2002**, *114*, 4350−4386. (k) Trost, B.; van Vranken, D. L. *Chem. Rev.* **1996**, *96*, 395−422. (l) Grushin, V. V. *Organometallics* **2000**, *19*, 1888−1900. (m) Cabri, W.; Candiani, I.; DeBernardinis, S.; Francalanci, F.; Penco, S. *J. Org. Chem.* **1991**, *56*, 5796−5800. (n) Cabri, W.; Candiani, I. *Acc. Chem. Res.* **1995**, *28*, 2−7. (o) Brown, J. M.; Cooley, N. A. *Organometallics* **1990**, *9*, 353−359.

(2) Rouhi, A. M. *Chem. Eng. News* **2004**, *82*(36), 59−61.

(3) Amatore, C.; Jutand, A.; Medeiros, M. J.; Mottier, L. *J. Electroanal. Chem.* **1997**, *422*, 125−132.

(4) Amatore, C.; Azzabi, M.; Jutand, A. *J. Am. Chem. Soc.* **1991**, *113*, 8375−8384.

(5) Amatore, C.; Jutand, A.; Suarez, A. *J. Am. Chem. Soc.* **1993**, *115*, 9531−9541.

10.1021/om050160p CCC: $30.25
Publication on Web 04/08/2005

Scheme 1. Consensus ("Textbook") Catalytic Cycles for the Cross-Coupling Reaction with an Anionic Nucleophile (a) and That Proposed in Refs 3−7 (b)

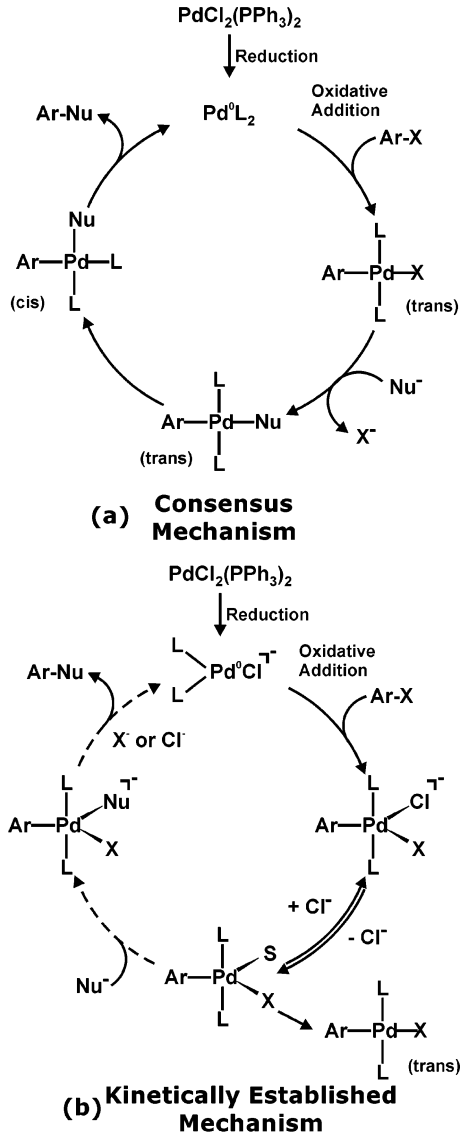

complex was dependent on the concentration of an additive anion, e.g., Cl^-. On the basis of this observation and other mechanistic indications, it was proposed that the catalytic cycle starts with a trivalent anionic complex,[4−7,9] as shown in Scheme 1b, and that this complex makes the cycle more efficient. While the presence of this intermediate and the pentavalent anionic Pd(II) ones, etc., were proposed by various mechanistic criteria, still, none of these transient species could be characterized structurally. Therefore, the proposed "anionic" cycle in Scheme 1b was viewed as the minimum kinetic requirement and the structures in it as tentative suggestions on the basis of kinetic, ^{31}P NMR, and electrochemical information. Since then, the

Chart 1. $L_2Pd^0-X^-$ Complexes Studied in Ref 10

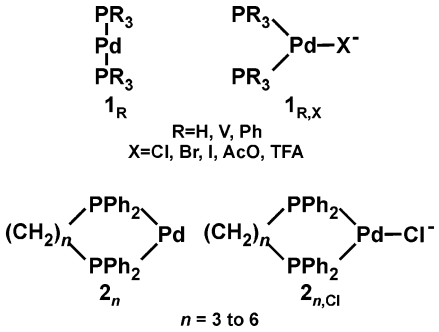

authors of the present paper have established theoretically the validity of the structure proposed for the trivalent anionic Pd(0).[10] Thus, the chloride additive is not a mere curiosity, especially so since it is potentially the cause that makes the catalytic cycle more efficient.

This suggestion is intriguing: *why should an apparently innocuous additive have any impact on the catalytic cycle*? Led by this question and by the more general one appearing in the title, it was deemed necessary to tackle the problem using theoretical means. This is the main focus of the present paper, which seeks an understanding of the impact of the additive on the catalytic cycle of the cross-coupling reaction, as a model for all these transformations that involve Pd(0) catalysts.

As mentioned already, our recent density functional theoretical (DFT) investigation[10] demonstrated for the first time that these novel tricoordinated $Pd^0L_2X^-$ complexes are stable species that exist even in solvents such as THF. A variety of ligands, shown in Chart 1 (L = PPh_3, PV_3 (V = vinyl), PH_3, bidentate phosphine ligands; X = Cl, Br, I, AcO, TFA), were studied in order to establish the stability patterns of the complex. The stability of the Pd−X^- bond was shown to depend on (a) the electron donor capability of X^-, and its ability for back-bonding into the empty 5p orbitals of the Pd(0) center, (b) the nature of the phosphine ligands, their ability to withdraw electrons from the Pd(0) center, and (c) the methylene chain length, $(CH_2)_n$, of the bidentate phosphane ligand. Especially interesting was the finding that the strongest Pd−X^- bonds were calculated for the bidentate ligand with the shortest methylene chain, $n = 3$. Thereafter, the bond energy decreased and, for $n = 6$, was almost identical with that in the case of L = PPh_3. All these trends were shown to have simple rationales in the respective orbital interaction diagram.[11,12]

Following the theoretical characterization of the putative active species of the zerovalent palladium catalyst, it was deemed necessary to carry out a theoretical study with an aim to assess the relative efficiency of the two catalytic cycles for the cross-coupling reaction in Scheme 1b. Therefore, one focus of our study is the comparison of the oxidative addition step using Pd^0L_2 (the consensus mechanism) and $Pd^0L_2Cl^-$ (the mechanism in Scheme 1b) as the active catalyst forms. As a substrate we selected phenyl chloride (Ph−Cl), since the oxidative

(6) Amatore, C.; Jutand, A. *J. Organomet. Chem.* **1999**, *576*, 254−278.
(7) Amatore, C.; Jutand, A. *Acc. Chem. Res.* **2000**, *33*, 314−321.
(8) Amatore, C.; Jutand, A.; Lemaitre, F.; Ricard, J. L.; Kozuch, S.; Shaik, S. *J. Organomet. Chem.* **2004**, *689*, 3728−3734.
(9) Some anionic tricoordinated Pt complexes were studied by: Chicote, M. T.; Green, M. G.; Spencer, J. L.; Stone, F. G. A.; Vicente, J. *J. Chem. Soc., Dalton Trans.* **1979**, 536.
(10) Kozuch, S.; Shaik, S.; Jutand, A.; Amatore, C. *Chem. Eur. J.* **2004**, *10*, 3072−3080.
(11) Hoffmann, R. *Science* **1981**, *211*, 995−1002.
(12) Albright, T. A.; Burdett, J. K.; Whangbo, M. H. *Orbital Interactions in Chemistry*, Wiley-Interscience: New York, 1985.

Scheme 2. Oxidative Addition Reactions of Pd^0L_2 and $Pd^0L_2Cl^-$ and the Catalytic Cycles Investigated in This Study

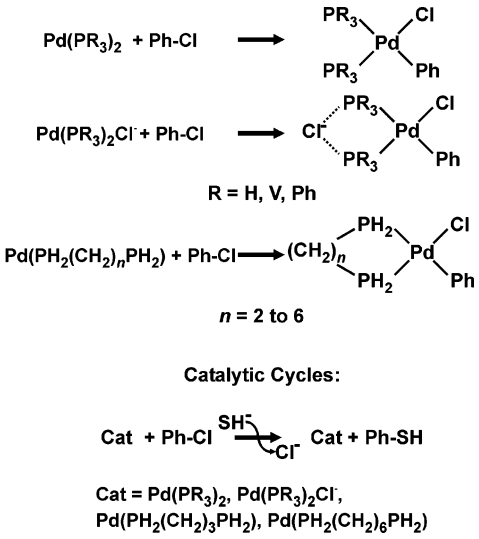

addition of phenyl chloride is often the rate-limiting step in palladium-catalyzed cross-coupling reactions.[1g,h,j] Recent calculations by Lin et al. for the related Heck reaction,[13a] using $Pd(PH_3)_2$ as a catalyst, showed that the rate-limiting step is oxidative addition, while the rest of the cycle is mainly downhill in a rather smoother path. The only study that compares the efficacy of the pristine and anionic catalysts is the recent paper of Goossen et al.,[13b] which communicated DFT calculations of the oxidative addition of $Pd^0(PMe_3)_2(OAc)^-$ to phenyl iodide in the gas phase. No study has as yet compared *the entire catalytic cycles* of the pristine and anionic catalysts. This issue is treated in the present paper, which looks at a variety of other issues of the cross-coupling reaction, as detailed below.

Since the bidentate phosphine ligands $R_2P(CH_2)_nPR_2$ ($n = 2-6$) form rather stable anionic complexes,[10] and since the $Pd^0[R_2P(CH_2)_nPR_2]$ complexes are known to undergo oxidative addition with activation energies smaller than for a nonchelating ligand like PPh_3,[14] we compared the entire catalytic cycles also for two bidentate phosphane ligands, with an aim to assess the chelate effect. The oxidative addition processes and catalytic cycles that were studied are depicted in Scheme 2. We note that the choices of the substrate as Ph−Cl, the ligands as PH_3 and $PH_2(CH_2)_nPH_2$, and HS^- as the nucleophile were made to ascertain the efficiency of the computations; however, the activation of Ph−Cl under experimental conditions generally requires more specific ligation of the Pd(0) center.

The major focus of the paper is to seek an answer for the title question: *what makes for a good catalytic cycle?* To tackle this question, a short background is necessary.[6] Consider, in Figure 1, the velocity of an efficient

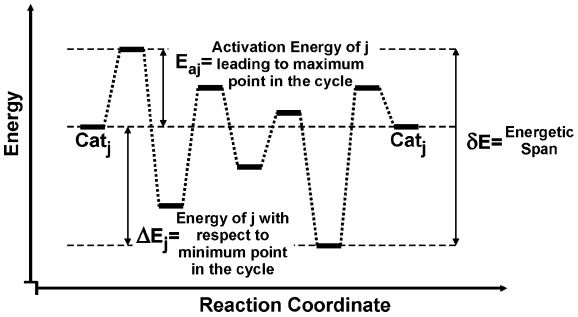

Figure 1. Schematic representation of a catalytic cycle. The factors that determine its efficiency are E_{aj} and δE.

catalysis when the kinetic steady state is reached. In this case, one can use the Arrhenius rate law and express the velocity of the cycle as

$$v \approx A \exp(-E_{aj}/RT)[Cat_j] \quad (1)$$

where Cat_j is the catalyst species of the highest transition state and E_{aj} is the corresponding activation energy. A rough estimate of the concentration of Cat_j can be achieved by considering the respective Boltzmann distribution

$$[Cat_j] \approx [Cat_t] \exp(\Delta E_j/RT) \quad (2)$$

where ΔE_j is the energy of j with respect to the lowest lying intermediate and $[Cat_t]$ the total concentration of catalyst species. This leads to

$$v \approx A' \exp[-(E_{aj} + E_j)/RT] = A' \exp(-\delta E/RT) \quad (3)$$

Here δE is *the energetic span of the cycle*, which by reference to Figure 1 is the difference between the highest and the lowest points of the catalytic cycle. This factor determines the frequency of the catalytic cycle, namely *the turnover number* (cycles per second).[15] Therefore, a good catalytic cycle must consist of low-lying transition states with high-lying intermediates. Exporting this idea to the problem at hand, we shall seek to define the role of the Cl^- additive; does it really bring any advantage regarding the energy barrier for oxidative addition and the energy span of the cycle?

Computational Methods

Ideally the study should have included the effect of a solvent (THF). However, a detailed study of Cl^- in THF showed the polarizable continuum model (PCM) greatly overestimates the solvation energy of Cl^-, leading to a solvation energy of 136 kcal/mol, compared with an estimate of 64 kcal/mol.[14d] For $Cl^-(THF)_{7-10}$ embedded in PCM, we calculated a solvation energy of 71 kcal/mol,[10] which gets closer to the estimated experimental data. Thus, a realistic solvation model that accounts for long-range interactions would have to involve an explicit cluster of 10 or more THF molecules, all embedded in a polarized continuum solvent (see the Supporting Information). Such a study of the entire catalytic cycle is too extensive at present. Therefore, rather than introducing errors through inappropriate solvation models, we preferred to explore at present the catalytic cycle in a gas-phase situation, with due

(13) (a) Lin, B.; Liu, L.; Fu, Y.; Luo, S.; Chen, Q.; Guo, Q. *Organometallics* **2004**, *23*, 2114−2123. (b) Goossen, L. J.; Koley, D.; Hermann, H.; Thiel, W, *Chem. Commun.* **2004**, 2141−2143.

(14) For computational work on the chelate effect see: (a) Su, M.; Chu, S. *Inorg. Chem.* **1998**, *37*, 3400−3406. (b) Sakaki, S.; Biswas, B.; Sugimoto, M. *J. Chem. Soc., Dalton Trans.* **1997**, 803−809. (c) For experimental work on the chelate effect: Portnoy, M.; Milstein, D. *Organometallics* **1993**, *12*, 1665−1673. (d) For a recent DFT study of the oxidative addition using a chelated Pd(0) with a diphoshane ligand, see: Senn, H. M.; Ziegler, T. *Organometallics* **2004**, *23*, 2980.

(15) As pointed out by a reviewer, reducing the energy span does not always bring advantage to a catalytic cycle, e.g., in cases where there are a few preequilibrium steps and the intermediate product after the highest transition state is unstable relative to the species in the first steps. This is not the case in the present cycles.

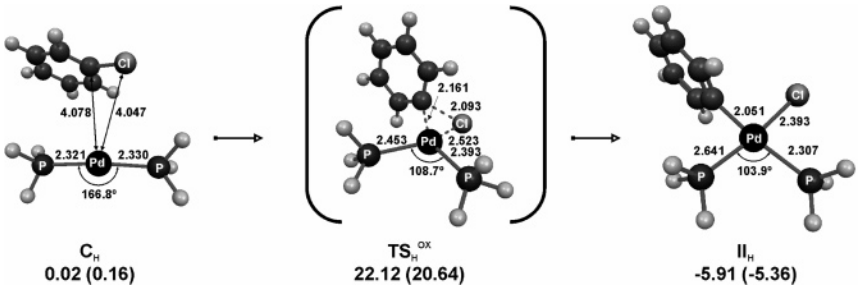

Figure 2. Mechanism describing the oxidative addition of PhCl to $\mathbf{1}_{H}$. All energies (in kcal/mol) are indicated relative to the reactants. Values in parentheses include zero point energy (ZPE) correction.

caution regarding the conclusions. We verified, however, two crucial points, which ascertain that the key features of the gas-phase cycle should carry over to the reaction in a solvent: (a) that the tricoordinate complex persists in solution[10] (using PCM and a cluster of THF molecules embedded in a continuum) and (b) that the Cl^- that is coordinated to the phosphines in the bond activation transition state ($\mathbf{TS}_{H,Cl}^{Ox,Back}$; Figures 5 and 6) does not dissociate when the TS is embedded in a cluster of seven THF molecules.

The study used density functional theory (DFT) with the hybrid functional B3LYP throughout. This hybrid functional is considered as a reliable method for large molecules, especially when transition metals are included.[16]

Previous studies[10] showed that the use of phosphine (PH_3) molecules as ligands produces model complexes that have properties roughly comparable to those of the experimental system with the phenylphosphine ligand (with the exception of steric repulsions). Therefore, as shown in Scheme 2, we used as catalyst species the small model systems $Pd(PH_3)_2$ ($\mathbf{1_H}$), $Pd(PH_3)_2Cl^-$ ($\mathbf{1_{H,Cl}}$), and $Pd[H_2P(CH_2)_nPH_2]$ ($\mathbf{2}_{H,n}$). To model more realistic systems, the oxidative addition step was studied also with $\mathbf{1}_V$, $\mathbf{1}_{Ph}$, $\mathbf{1}_{V,Cl}$, and $\mathbf{1}_{Ph,Cl}$ ($Pd(PV_3)_2$, $Pd(PPh_3)_2$, and their respective anionic complexes).

For the smaller catalyst models ($\mathbf{1}_H$), we used for both geometry and energy an effective core potential double-ζ polarized basis set augmented with diffuse functions, LACVP**+-(Pd)-6-31+G*(rest), implemented in JAGUAR 4.2[17] (shorthand notation, LACVP**+//LACVP**+). For the larger systems $\mathbf{1}_V$, $\mathbf{1}_{V,Cl}$, $\mathbf{1}_{Ph}$, and $\mathbf{1}_{Ph,Cl}$, the geometry optimization was done with the double-ζ polarized basis set LACVP*(Pd)-6-31G*(rest), followed by energy calculation at a larger basis set that includes the diffuse function: hence, LACVP**+//LACVP*. A benchmark study of basis sets[10] showed that the LACVP**+// LACVP* level led to errors smaller than 1 kcal/mol compared to higher level basis sets. Frequency calculations were carried out with Gaussian 98[18] in the same basis set of the geometry optimization and were used to test for genuine minima and transition states and for the estimation of zero point energy corrections. All charges were calculated with the Mulliken population analysis.

The calculations generated a multitude of data. To save space, many of these data are relegated to the Supporting Information (*xyz* structures), while the discussion contains only key information.

Results

As noted above, the rate-controlling step of the cross-coupling reaction involving Ph−Cl as substrate is the oxidative addition. This step was studied in great detail using different catalyst models for the two alternative cycles of Scheme 1. In the following subsections, we described first the consensus mechanism using the neutral catalysts $\mathbf{1}_H$ and the chelated ones $\mathbf{2}_{H,n}$ (n = 2−6). Subsequently, we describe the reaction mechanism of the anionic catalysts $\mathbf{1}_{H,Cl}$, $\mathbf{1}_{V,Cl}$, and $\mathbf{1}_{Ph,Cl}$. Finally, after establishing the appropriateness of the smaller catalysts models, we present the full catalytic cycles for the catalysts $\mathbf{1}_{H,Cl}$, $\mathbf{1}_H$, and $\mathbf{2}_{H,n}$ (n = 2−6).

A. Oxidative Addition in the Consensus Mechanism. (a) Oxidative Addition of $\mathbf{1}_H$. Figure 2 shows the energy profile and critical species of the oxidative addition reaction of $Pd(PH_3)_2$ ($\mathbf{1}_H$) with chlorobenzene, Ph−Cl. The approach of the catalyst to the substrate leads to a cluster ($\mathbf{C}_H$). The interaction between the reactants is seen to be negligible. The oxidative addition occurs by a concerted Pd insertion into the C−Cl bond of Ph−Cl, via a transition state, $\mathbf{TS}_H^{ox}$, which lies 22.12 kcal/mol (20.64 kcal/mol with ZPE correction) above the reactants. Interestingly, the structure of $\mathbf{TS}_H^{ox}$ has Pd- - -C, Pd- - -Cl, and C- - -Cl bond distances similar to those reported[14d] for the reactions of $\mathbf{2}_{Me,2}$ with phenyl halides in THF (using a continuum model). The oxidative addition product $(PH_3)_2Pd^{II}$[Cl,Ph] is a square-planar complex labeled as $\mathbf{II_H}$, and the reaction is slightly exothermic.

(b) Oxidative Addition of the Chelated Catalysts $\mathbf{2}_{H,n}$. The oxidative addition mechanism of the chelated palladium catalysts has similarities with and differences from that shown above in Figure 2. As before, all of the reactions involve an initial cluster, $\mathbf{C}_{H,n}$, a transition state, $\mathbf{TS}_{H,n}^{ox}$, and an oxidative addition product, $\mathbf{II}_{H,n}$. However, unlike before, there are now additional inter-

(16) For computational work on organometallic species, including Pd, using DFT and other methods, see for example: (a) Niu, S.; Hall, M. B. *Chem. Rev.* **2000**, *100*, 353−405. (b) Sundermann, A.; Uzan, O.; Martin, J. M. L. *Chem. Eur. J.* **2001**, *7*, 1703−1711. (c) Dedieu, A. *Chem. Rev.* **2000**, *100*, 543−600. (d) Goldfuss, B.; Kazmaier, U. *Tetrahedron* **2000**, *52*, 6493−6496. (e) Straub, B. F. *J. Am. Chem. Soc.* **2002**, *124*, 14195-14201. (f) Albert, K.; Gisdakis, P.; Rösch, N. *Organometallics* **1998**, *17*, 1608−1616. (g) Frenking, G.; Fröhlich, N. *Chem. Rev.* **2000**, *100*, 717−774. (h) Koga, N.; Morokuma, K. *Chem. Rev.* **1991**, *91*, 823−842. (i) Jakt, M.; Johnissen, L.; Rzepa, H. S.; Widdowson, D. A.; Wilhelm, R. *J. Chem. Soc., Perkin Trans. 2* **2002**, 576. (j) Bickelhaupt, F. M.; Ziegler, T.; Schleyer, P. v. R. *Organometallics* **1995**, *14*, 2288. (k) Deeth, R. J.; Smith, A.; Brown, J. M. *J. Am. Chem. Soc.* **2004**, *126*, 7144−7151. (l) Cundari, T. R.; Deng, J.; Zhao, Y. *J. Mol. Struct. (THEOCHEM)* **2003**, *632*, 121−129.

(17) Jaguar 4.2; Schrödinger, Inc., Portland, OR, 1991−2000.

(18) Frisch, M. J.; Trucks, G. W.; Schlegel, H. B.; Scuseria, G. E.; Robb, M. A.; Cheeseman, J. R.; Zakrzewski, V. G.; Montgomery, J. A., Jr.; Stratmann, R. E.; Burant, J. C.; Dapprich, S.; Millam, J. M.; Daniels, A. D.; Kudin, K. N.; Strain, M. C.; Farkas, O.; Tomasi, J.; Barone, V.; Cossi, M.; Cammi, R.; Mennucci, B.; Pomelli, C.; Adamo, C.; Clifford, S.; Ochterski, J.; Petersson, G. A.; Ayala, P. Y.; Cui, Q.; Morokuma, K.; Malick, D. K.; Rabuck, A. D.; Raghavachari, K.; Foresman, J. B.; Cioslowski, J.; Ortiz, J. V.; Stefanov, B. B.; Liu, G.; Liashenko, A.; Piskorz, P.; Komaromi, I.; Gomperts, R.; Martin, R. L.; Fox, D. J.; Keith, T.; Al-Laham, M. A.; Peng, C. Y.; Nanayakkara, A.; Gonzalez, C.; Challacombe, M.; Gill, P. M. W.; Johnson, B. G.; Chen, W.; Wong, M. W.; Andres, J. L.; Head-Gordon, M.; Replogle, E. S.; Pople, J. A. *Gaussian 98*, revision A.11.2; Gaussian, Inc.: Pittsburgh, PA, 1998.

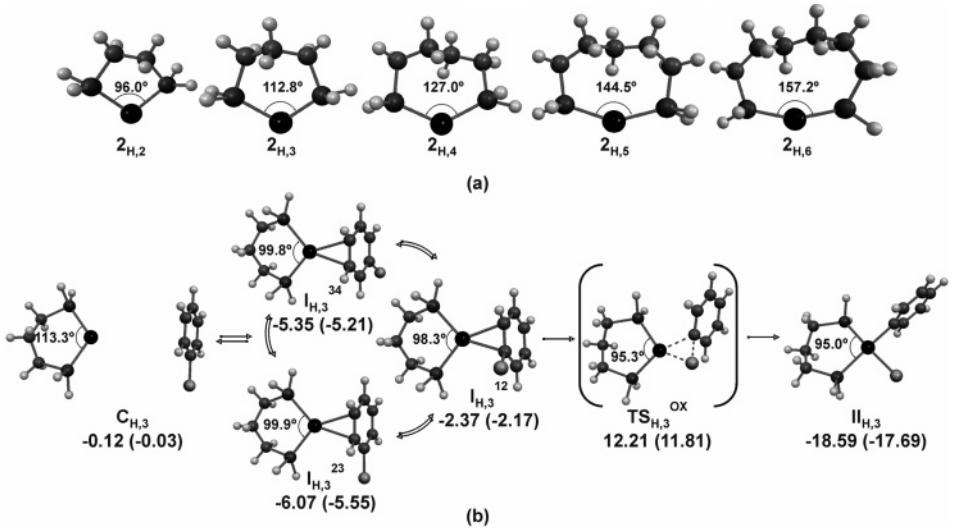

Figure 3. (A) The $\mathbf{2}_{H,n}$ catalysts studied. (b) Example of the oxidative addition of PhCl with $\mathbf{2}_{H,3}$. The energy values in kcal/mol are relative to the reactants (zero point energy in parentheses). The η^2-type complexes are labeled according to their position relative to the ipso carbon of PhCl.

Table 1. Relative Energies of Transition States ($TS_{H,n}^{ox}$), and Products ($II_{H,n}$) of the Oxidative Addition Reaction of $\mathbf{2}_{H,n}$ with PhCl[a]

	$TS_{H,n}^{ox}$	$II_{H,n}$
$\mathbf{2}_{H,2}$	9.65 (9.07)	−19.25 (−18.47)
$\mathbf{2}_{H,3}$	12.21 (11.81)	−18.59 (−17.69)
$\mathbf{2}_{H,4}$	17.16 (15.97)	−14.68 (−14.24)
$\mathbf{2}_{H,5}$	19.08 (18.36)	−10.41 (−9.44)
$\mathbf{2}_{H,6}$	21.57 (20.87)	−8.48 (−7.58)

[a] Energy units in kcal/mol relative to the reactants (ZPE corrected values in parentheses).

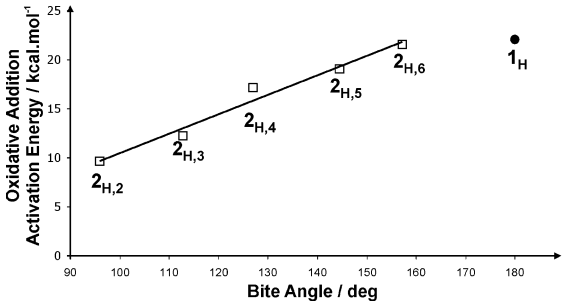

Figure 4. Plot of the oxidative addition barriers vs the bite angle (P−Pd−P) of the diphosphine ligand in $\mathbf{2}_{H,n}$. The corresponding data point for $\mathbf{1}_H$, for which the P−Pd−P angle is 180°, is also displayed.

mediates where the palladium catalysts form η^2-type complexes with Ph−Cl. As noted above, here too the structure of $\mathbf{TS}_H^{ox}$ has Pd- - -C, Pd- - -Cl, and C- - -Cl bond distances (2.166, 2.532, and 2.074 Å, respectively, for $n = 3$; for other distances see Table S.1 in the Supporting Information) similar to those reported by Sen and Ziegler[14d] for the reactions of $\mathbf{2}_{Me,2}$ with phenyl halides in THF; these authors have also reported η^2 complexes. To save space, we have collected in Table 1 the relative energy values of the corresponding critical points ($\mathbf{TS}_{H,n}^{ox}$ and $\mathbf{II}_{H,n}$), and we show the complete mechanism for $\mathbf{2}_{H,3}$ in Figure 3.

Inspection of Table 1 shows that the activation energy of the oxidative addition now depends critically on the length of the methylene chain in the diphosphine ligand of the catalyst, $\mathbf{2}_{H,n}$. Figure 4 shows the correlation between the barriers and the P−Pd−P angle (the bite angle) of the diphosphine ligand. It is seen that as the bite angle increases from 96.0° in $n = 2$ to 157.2° in $n = 6$, the barrier increases from 9.65 to 21.57 kcal/mol and becomes roughly equal to the barrier of the $\mathbf{1}_H$ catalyst, where the bite angle is 180°. From Table 1, it is possible to see that the reduction of the barrier along the series of the bidentate ligands parallels the increase of stability of the oxidative addition product.

The η^2-type complexes in Figure 3 merit a brief description. The same effect that was found to be responsible for the stability of the Pd−Cl$^-$ bond in the chelate complexes[10] is responsible now for the occurrence of the η^2-type complexes en route to oxidative addition. This factor, pointed out before by Sakaki et al.,[14b] is the inability of the chelated complexes to relax the P−Pd−P angle to 180°. When the Pd^0L_2 complex is unable to relax the P−Pd−P angle to 180°, the bond-dissociated fragment is relatively unstable (see Figure 9 below), and hence, the Pd−Cl$^-$ bond dissociation energy becomes larger, compared with the pristine fragment that relaxes the angle.[10] For the same reason, the chelated Pd^0L_2 fragment can form a stable bond, such as in the η^2-type complexes to Ph−Cl. Since the unused relaxation energy of the Pd^0L_2 fragment depends on the length of the methylene chain in the bidentate ligand, the stability of the η^2 complexes depends strongly on the chain length. Thus, only the most stable intermediates ($\mathbf{I}_{H,n}^{23}$ and $\mathbf{I}_{H,n}^{34}$; the superscripts indicate positions relative to the ipso carbon in Ph−Cl) were found for all the bidentate complexes, whereas the less stable intermediate ($\mathbf{I}_{H,n}^{12}$) was located only for $n = 2$, 3 (see the Supporting Information).

B. Oxidative Addition of the Anionic Complexes (Scheme 1b). (a) Oxidative Addition of the Anionic Catalyst $\mathbf{1}_{H,Cl}$. Unlike the neutral catalyst species, $\mathbf{1}_H$, the anionic tricoordinated complex exhibits a multistep mechanism. The results displayed in Figure 5 resemble those found for the oxidative addition of the anionic catalyst $Pd^0(PMe_3)_2(OAc)^-$ to phenyl iodide.[13b] The cluster $\mathbf{C}_{H,Cl}$ in Figure 5 is considerably more stable than the free reactants by −8.29 kcal/mol. Subse-

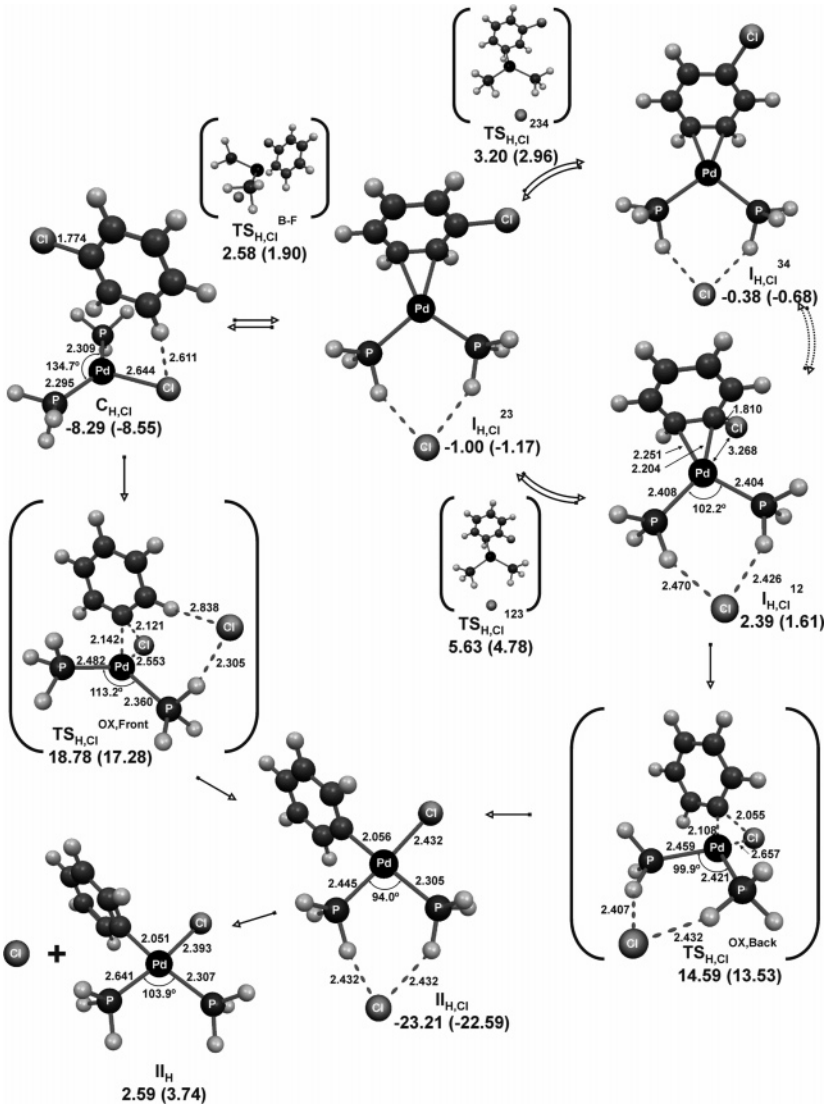

Figure 5. Mechanism of oxidative addition of PhCl with $\mathbf{1}_{H,Cl}$ (transition states in brackets). The values under the species correspond to relative energies in kcal/mol. In parentheses are given the values corrected by zero point energies (ZPEs).

quently, as the reactants approach one another, an η^2 complex, labeled as $\mathbf{I}_{H,Cl}{}^{23}$, is formed. This is followed by rearrangement of the η^2 complexation to form finally the $\mathbf{I}_{H,Cl}{}^{12}$ complex that leads to the transition state $\mathbf{TS}_{H,Cl}{}^{x,Back}$. The activation energy relative to the free reactants is 14.59 kcal/mol, 7.5 kcal/mol lower than the corresponding value for the neutral pathway.[19] Starting with the η^2 complex and onward, it is apparent that palladium is reluctant to form pentacoordinated complexes, and the coordination of Ph−Cl to the palladium causes the dissociation of the original Pd−Cl^- bond. The dissociated Cl^- moves, in turn, to the position between the phosphine ligands, where the positively charged hydrogens attract it; a similar behavior of the anionic additive is apparent in the results of Thiel and coworkers.[13b] The Coulomb caging of the Cl^- is illustrated in Figure 6 (some charge transfer is also apparent). The interaction of Cl^- with the transition state is significant and is calculated to be 17 kcal/mol. This interaction energy is at least of the same magnitude as the Pd−Cl^- bond energy in the anionic catalyst. Indeed, when the transition state $\mathbf{TS}_{H,Cl}{}^{ox,Back}$ was embedded in a cluster of seven THF's and subjected to geometry optimization of the solvent molecules and the chloride anion, the distances between the Cl^- and the phosphines got somewhat longer (by 0.27 and 0.43 Å) relative to the gas-phase structure, but the anion remained between the phosphines and did not dissociate to be embedded in the $(THF)_7$ cluster (see the Supporting

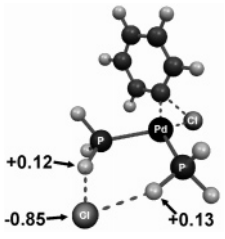

Figure 6. Mulliken charges in $\mathbf{TS}_{H,Cl}{}^{ox,Back}$ showing the Coulomb caging of Cl^- by the phosphine ligands.

(19) It is possible to infer qualitatively the activation energy of $\mathbf{1}_{H,Cl}$ by considering the series of η^2 intermediates. The $\mathbf{I}_{H,n}{}^{12}$ complex is stable only when n is **2** or **3**. The other two intermediates, $\mathbf{I}_{H,n}{}^{23}$ and $\mathbf{I}_{H,n}{}^{34}$, are stable for all the chelate complexes. For $\mathbf{1}_{H,Cl}$ the three intermediates are stable, due to the chelating effect of the Cl^- on the phosphine ligands in $\mathbf{TS}_{H,Cl}{}^{x,Back}$. Note that for the pristine catalyst, $\mathbf{1}_H$, none of the three η^2 structures could be located. From here we can deduce that the anionic $\mathbf{1}_{H,Cl}$ will have at least a lower transition state than $\mathbf{2}_{H,4}$ and $\mathbf{1}_H$ will have a higher activation energy than $\mathbf{2}_{H,6}$.

Table 2. Relative Energies of the Species along the Oxidative Addition Pathways of $\mathbf{1}_{V,Cl}$ vs $\mathbf{1}_V$ and $\mathbf{1}_{Ph,Cl}$ vs $\mathbf{1}_{Ph}$[a]

	energy (kcal/mol)			energy (kcal/mol)	
	PdL_2Cl^-	PdL_2		PdL_2Cl^-	PdL_2
C_H	−8.29	0.02	II_V	−11.17	−0.08
TS_H^{ox}	14.59	22.12	C_{Ph}	−5.04	−1.64
II_H	−23.21	−5.91	TS_{Ph}^{ox}	26.08	30.34
C_V	−6.16	−0.57	II_{Ph}	13.57	1.39
TS_V^{ox}	21.48	24.60			

[a] The labels of the species correspond to the cluster (**C**), the oxidative transition state (**TS**), and the Pd(II) product (**II**). The subscripts V and Ph represent the vinyl and phenyl substituents on the phosphine, respectively.

Information). Furthermore, the solvation energy of the TS was calculated to be 38.7 kcal/mol, compared with 34.7 kcal/mol for bare Cl^-. This indicates that the interaction between the Cl^- anion and the phosphine ligands is of the same order of magnitude as with solvent molecules. It is therefore not unreasonable to expect that the interaction of Cl^- with the phosphine ligands will be maintained also in a solvent.

The preference of the Cl^- for its coordination to the phosphine ligand is apparent from the alternative transition state $\mathbf{TS}_{H,Cl}^{ox,Frnt}$ in Figure 5, which lies 4.2 kcal/mol higher than $\mathbf{TS}_{H,Cl}^{ox,Back}$. There seems to be some importance to the position of the Cl^- in the transition state. Part of this advantage is associated again with the P−Pd−P angle. It is apparent that in $\mathbf{TS}_{H,Cl}^{ox,Back}$ the backside Cl^- keeps the angle considerably smaller than in $\mathbf{TS}_{H,Cl}^{OX,Frnt}$; the latter species resembles more the $\mathbf{TS}_H^{ox}$ species of the pristine catalyst, $\mathbf{1}_H$. Note, however, that in any case the barrier of the anionic catalyst is smaller than that for the $\mathbf{1}_H$ catalyst (see Figure 2).[19]

C. Results for the Realistic Models ($\mathbf{1}_{V,Cl}$, $\mathbf{1}_{Ph,Cl}$). To compare the alternative cycles in Scheme 1 for more realistic catalysts, we calculated the oxidative additions of Ph−Cl to $Pd(PV_3)_2Cl^-$ ($\mathbf{1}_{V,Cl}$, V = vinyl) and $Pd(PPh_3)_2Cl^-$ ($\mathbf{1}_{Ph,Cl}$) and compared them to those of their respective neutral dicoordinated complexes ($\mathbf{1}_V$ and $\mathbf{1}_{Ph}$). The respective mechanisms resemble those of the simple catalysts, $\mathbf{1}_{H,Cl}$ and $\mathbf{1}_H$ (Figures 2 and 5 above). The relative energies of the species incurred in these processes are shown in Table 2, while the corresponding **TS** structures are depicted in Figure 7. The rest of the data can be found in the Supporting Information.

It is apparent that the simple catalysts mimic the more realistic systems. While the effect on the barrier is smaller than in the simplified model, still with the experimental reagent the barrier is reduced by a significant 4.2 kcal/mol (corresponding to 3 orders of magnitude in rate). Importantly, as before, the anionic additive migrates to the back of the complex and gets stabilized by electrostatic interactions with the substituents of the phosphine ligands. The presence of Cl^-, in turn, causes the P−Pd−P angle to shrink slightly and the oxidative addition barrier is lowered.

D. Catalytic Cycle for the Various Catalysts. Due to the similar actions of the small catalyst model and the larger catalyst model, the former was deemed an appropriate model for the rest of the cycle. Following the oxidative addition, the cycle continues with characteristic steps, which involve nucleophilic substitution

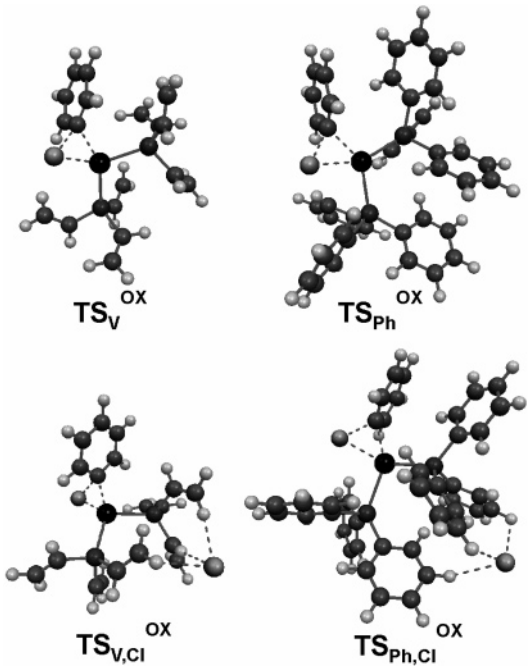

Figure 7. TS structures for the oxidative additions of $\mathbf{1}_{V,Cl}$, $\mathbf{1}_V$, $\mathbf{1}_{Ph,Cl}$, and $\mathbf{1}_{Ph}$.

and formation of the substitution product; the nucleophile of choice in this study is SH^-, and hence the net reaction is the conversion of Ph−Cl to Ph−SH (see Scheme 2). The characteristic cycles are depicted in Figure 8; part a describes the cycle for the $\mathbf{1}_H$ and $\mathbf{1}_{H,Cl}$ catalysts, while part b describes the cycle for $\mathbf{2}_{H,n}$ (n = 3, 6). Table 3 collects the relative energies of the various species and the energetic span values, δE, for these catalysts.

All the mechanisms start with oxidative addition, followed by nucleophilic substitution and terminated by reductive elimination of the Ph−SH product. In all the cycles in Figure 8, the favorable approach of the nucleophile is from the back side of the complex, where Coulomb caging occurs. In the case of $\mathbf{1}_H$, it was found that the nucleophile initially displaces a PH_3 ligand (see $\mathbf{II}_L$ in Figure 8a) followed by the substitution of Cl^- with the initially displaced PH_3 (see $\mathbf{II}'_{Cl}$). For $\mathbf{2}_{H,3}$ and $\mathbf{2}_{H,6}$ in Figure 8b, there is a direct substitution of Cl^- by SH^-. The cycle of the anionic catalyst, in Figure 8a, involves a succession of η^2 intermediates en route to the oxidative addition transition state $\mathbf{TS}_{H,Cl}^{ox}$. A similar succession is observed for the chelated catalyst $\mathbf{2}_{H,3}$ in Figure 8b. By comparison, the cycles of the pristine catalyst and the chelated catalyst with the largest ring, $\mathbf{2}_{H,6}$, are similar and have fewer intermediate structures.

There are, however, some fundamental features, which characterize the cycle of the anionic catalyst in Figure 8a. The original chloride anion (indicated as $*Cl^-$) remains bound to the palladium catalyst all the way up to the nucleophilic substitution step. While we could not locate any pentacoordinate intermediate complexes, we note that the additive is present in the complex (e.g., $\mathbf{II}_{H,Cl}$), which has a stoichiometry identical with that of a pentacoordinate palladium complex. The reluctance of palladium to form a pentacoordinated complex is well documented.[13b,16b,20] In this respect the present results are in good accord with the study of Goossen, Thiel, and co-workers,[13b] who could not locate

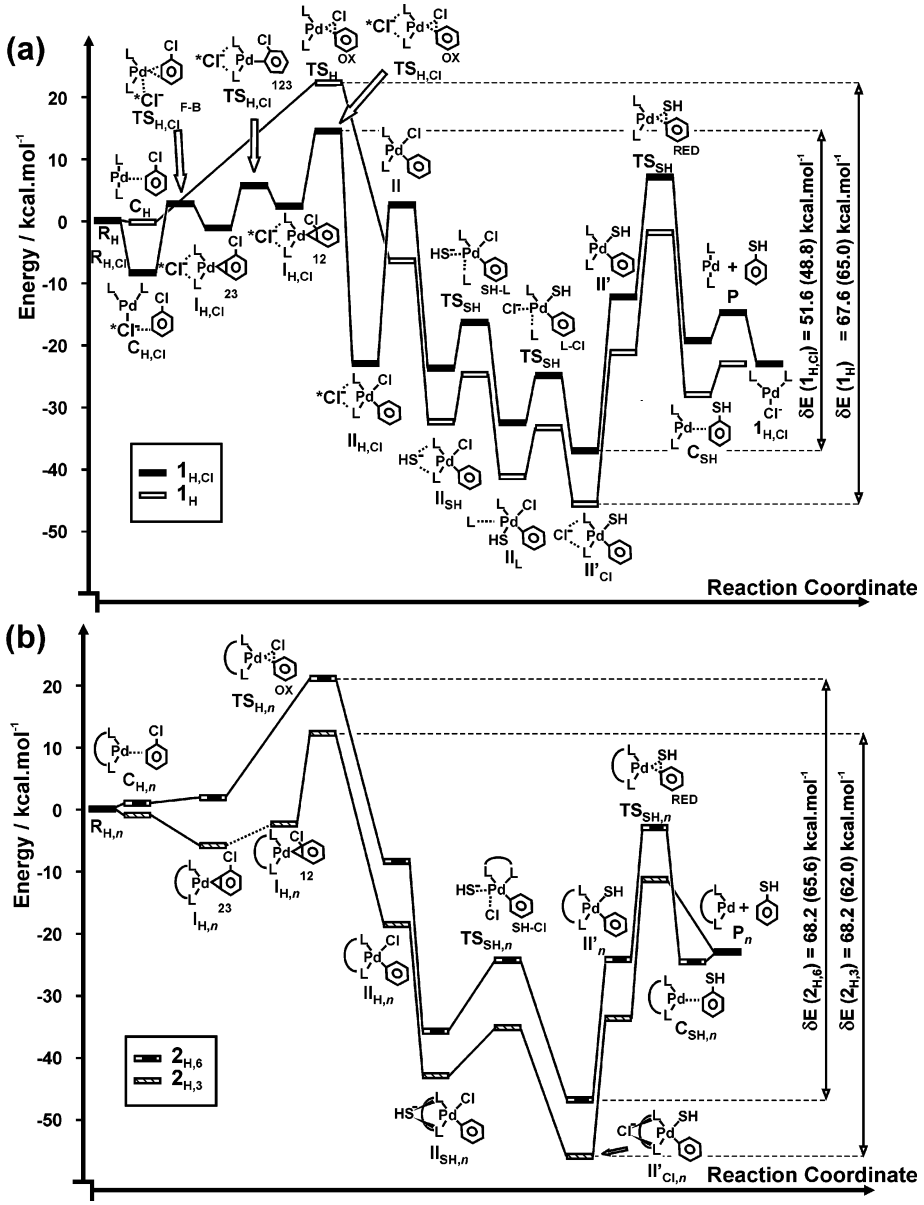

Figure 8. Full catalytic cycles for (a) $\mathbf{1}_{H}$ and $\mathbf{1}_{H,Cl}$ and (b) $\mathbf{2}_{H,3}$ and $\mathbf{2}_{H,6}$. Only the most relevant structures of the η^2 intermediates are shown (these structures are not stable for $\mathbf{1}_{H}$). The quantities δE correspond to the energy span of the cycle (energy values in parentheses involve ZPE correction). Note that the reactants for the two cycles are placed together at zero energy. Consequently, the relative energies of other species are different in the two cycles even when the species are identical.

a pentacoordinated complex in the oxidative addition of $Pd^0(PMe_3)_2(OAc)^-$ to phenyl iodide.

As the nucleophilic-substitution phase begins, the nucleophile SH^- initially displaces the chloride ion additive and forms a prenucleophilic substitution intermediate with the SH^- nestled at the back of the palladium complex (see $\mathbf{II}_{H,Cl} \rightarrow \mathbf{II}_{SH}$ in Figure 8a). Subsequently, at the end of the substitution and after the product release, the anionic tricoordinated complex $\mathbf{1}_{H,Cl}$ is regenerated, ready for a restart. This presence−exit−entrance dance of the chloride ion additive plays a key role in the efficacy of the cycle. This role can be deduced by comparing the energy spans of the two cycles in Figure 8a; *with the chloride additive, the energy span is 16 kcal/mol lower in energy*. This substantial energetic reduction is due to the combined effects of the stabilization of the highest point of the cycle, the transition state for oxidative addition ($\mathbf{TS}_{H,Cl}^{ox}$ vs $\mathbf{TS}_{H}^{ox}$), and the loss of the stabilization of the lowest energy species in the cycle, the substitution product intermediate ($\mathbf{II}'_{Cl}$). Note that the species $\mathbf{II}'_{Cl}$ is the same for the two cycles in Figure 8a; however, in the cycle of the anionic catalyst, the initial stabilization exerted by the additive in the catalyst, $\mathbf{1}_{H,Cl}$, is lost as the additive is displaced by the nucleophile. Thus, the destabilization of $\mathbf{II}'_{Cl}$ measures this loss relative to the reactant state, where the additive is present. In conclusion, the anionic catalyst, $\mathbf{1}_{H,Cl}$, is superior to the pristine species $\mathbf{1}_{H}$, since it flattens the energy landscape of the catalytic cycle, allowing thereby a larger turnover (eq 3) and, hence, a more efficient cycle. The loss of

(20) Hansson, S.; Norrby, P.-O.; Sjorn, M. P. T.; Åkermark, B.; Cuccholio, M. E.; Giordano, F.; Vitagliano, A. *Organometallics* **1993**, *12*, 4940. For enforced pentacoordination, see: Broring, M.; Brandt, C. D. *Chem. Commun.* **2003**, 2156.

Table 3. Relative Energies (in kcal/mol, ZPE in Parentheses) of the Species along the Oxidative Addition Pathways of $\mathbf{1}_{H,Cl}$, $\mathbf{1}_{H}$ and $\mathbf{2}_{H,n}$ (n = 2, 6)[a]

$\mathbf{1}_{H,Cl}$		$\mathbf{1}_{H}$		$\mathbf{2}_{H,3}$		$\mathbf{2}_{H,6}$	
$\mathbf{R}_{H,Cl}$	0.00 (0.00)	$\mathbf{R}_{H}$	0.00 (0.00)	$\mathbf{R}_{H,3}$	0.00 (0.00)	$\mathbf{R}_{H,6}$	0.00 (0.00)
$\mathbf{C}_{H,Cl}$	−8.29 (−8.55)	$\mathbf{C}_{H}$	0.02 (0.16)	$\mathbf{C}_{H,3}$	−0.12 (−0.03)	$\mathbf{C}_{H,6}$	−1.53 (−1.33)
$\mathbf{I}_{H,Cl}{}^{12}$	2.39 (1.61)	$\mathbf{I}_{H}{}^{12}$	not stable	$\mathbf{I}_{H,3}{}^{12}$	−2.37 (−2.17)	$\mathbf{I}_{H,6}{}^{12}$	not stable
$\mathbf{I}_{H,Cl}{}^{23}$	−1.00 (−1.17)	$\mathbf{I}_{H}{}^{23}$	not stable	$\mathbf{I}_{H,3}{}^{23}$	−6.07 (−5.55)	$\mathbf{I}_{H,6}{}^{23}$	2.06 (1.86)
$\mathbf{I}_{H,Cl}{}^{34}$	−0.38 (−0.68)	$\mathbf{I}_{H}{}^{34}$	not stable	$\mathbf{I}_{H,3}{}^{34}$	−5.35 (−5.21)	$\mathbf{I}_{H,6}{}^{34}$	2.41 (2.33)
$\mathbf{TS}_{H,Cl}{}^{OX}$	14.59 (13.53)	$\mathbf{TS}_{H}{}^{ox}$	22.12 (20.64)	$\mathbf{TS}_{H,3}{}^{ox}$	12.21 (8.08)	$\mathbf{TS}_{H,6}{}^{ox}$	21.57 (20.87)
$\mathbf{II}_{H,Cl}$	−23.21 (−22.59)						
II	2.59 (3.74)	**II**	−5.91 (−5.36)	$\mathbf{II}_{3}$	−18.59 (−17.69)	$\mathbf{II}_{6}$	−8.48 (−7.58)
$\mathbf{II}_{SH}$	−23.85 (−24.53)	$\mathbf{II}_{SH}$	−32.35 (−33.63)	$\mathbf{II}_{SH,3}$	−42.92 (−40.47)	$\mathbf{II}_{SH,6}$	−35.78 (−34.77)
$\mathbf{TS}_{SH}{}^{SH-L}$	−16.38 (−15.14)	$\mathbf{TS}_{SH}{}^{SH-L}$	−24.88 (−24.24)	$\mathbf{TS}_{SH,3}{}^{SH-Cl}$	−35.47 (−33.89)	$\mathbf{TS}_{SH,6}{}^{SH-Cl}$	−35.78 (−20.82)
$\mathbf{II}_{L}$	−32.60 (−30.30)	$\mathbf{II}_{L}$	−39.28 (−39.40)	$\mathbf{II'}_{Cl,3}$	−55.98 (−53.88)	$\mathbf{II'}_{Cl,6}$	−46.67 (−44.77)
$\mathbf{TS}_{SH}{}^{L-Cl}$	−24.88 (−15.14)	$\mathbf{TS}_{SH}{}^{L-Cl}$	−33.38 (−24.24)				
$\mathbf{II'}_{Cl}$	−36.99 (−35.24)	$\mathbf{II'}_{Cl}$	−45.49 (−44.34)				
II'	−12.20 (−10.08)	**II'**	−20.70 (−19.18)	$\mathbf{II'}_{3}$	−33.82 (−31.48)	$\mathbf{II'}_{6}$	−23.95 (−21.97)
$\mathbf{TS}_{SH}{}^{red}$	6.92 (7.81)	$\mathbf{TS}_{SH}{}^{red}$	−1.58 (−1.30)	$\mathbf{TS}_{SH,3}{}^{red}$	−11.34 (−9.85)	$\mathbf{TS}_{SH,6}{}^{red}$	−2.29 (−1.25)
$\mathbf{C}_{SH}$	−19.24 (−17.10)	$\mathbf{C}_{SH}$	−27.75 (−26.20)	$\mathbf{C}_{SH,3}$	not stable	$\mathbf{C}_{SH,6}$	−24.81 (−22.96)
P	−14.64 (−12.52)	**P**	−23.14 (−21.62)	$\mathbf{P}_{3}$	−23.14 (−21.62)	$\mathbf{P}_{6}$	−23.14 (−21.62)
$\mathbf{P}_{Cl}$	−23.14 (−21.62)						
E	51.6 (48.8)	**E**	67.6 (65.0)	**E**	68.2 (62.0)	**E**	68.2 (65.6)

[a] The barriers for the $\mathbf{2}_{H,n}$ catalysts decrease as n increases from 2 to 6 (see Figure 4).

stabilization, due to the departure of Cl^-, will be common also to the larger catalysts with phenyl and vinyl substituents on the phosphines. Thus, in each case, the anionic catalyst is expected to possess a flatter cycle with a smaller energy span relative to the pristine catalyst; e.g., the energetic advantage of $\mathbf{1}_{Ph,Cl}$ vis-á-vis $\mathbf{1}_{Ph}$ can be estimated as 10 kcal/mol or so (i.e., the sum of barrier reduction, of 4.2 kcal/mol, and the loss of the stabilization energy by the chloride[10]). This is precisely the role deduced initially from experiment.[7]

It is interesting to compare the cycle of the anionic catalyst to that of the chelated catalysts in Figure 8b. In agreement with previous conclusions,[14a−c] it is seen that the smaller chelating ligand, with n = 3, in Figure 8b lowers the transition state for the oxidative addition compared with that of the larger chelate, with n = 6. In fact, the oxidative addition barrier for $\mathbf{1}_{H,Cl}$ as catalyst (Figure 8a) is comparable to the barrier for $\mathbf{2}_{H,3}$. Thus, the Cl^- additive facilitates the oxidative addition and its action is effectively similar to the chelating effect of a small diphosphine chelate with n = 3. However, the similarity stops here, since the energy span quantities for $\mathbf{2}_{H,n}$ are seen to be large and virtually identical with one another, both being larger by 16.6 kcal/mol compared with the energy span of the anionic catalyst $\mathbf{1}_{H,Cl}$. Unlike the effect of the exit−entrance dance of the anionic catalyst, in the chelated complexes, the stabilizing effect brought by the reduction in the P−Pd−P angle carries over to the entire cycle; *it lowers the barriers and stabilizes the intermediates, thereby keeping a constant energy span similar to that of the pristine catalyst*.

Discussion

Our calculations reveal an intriguing effect of the anion additive in the catalytic reaction. This additive lowers the barrier for the rate-controlling oxidative addition step and destabilizes the product complex, thus reducing the energy span of the cycle.[15] *As such, the Cl^- additive effectively flattens the energy landscape of the cycle and thereby improves its turnover efficacy*. Since this is an important effect, generally in catalysis and specifically here, it is essential to understand its root causes. The following discussion addresses the effects of the additive on the oxidative addition barrier and on the nucleophilic addition product, the highest and lowest energy species in the cycles (see Figure 8).

A. Effect of the Additive on the Oxidative Addition Barrier. As we already noted, with regards to the barrier, the Cl^- additive mimics the effect of a chelating ligand with a small bite. Thus, as seen in Figure 4, in the series of the chelated catalysts ($\mathbf{2}_{H,n}$) the oxidative addition barrier decreases with the shortening of the methylene chain linking the phosphine moieties, which coordinate the palladium. In the case of the anionic complex, the Cl^- additive initially shrinks the P−Pd−P angle by coordinating to the Pd, and then it migrates in the transition state between the two phosphines and continues to keep a small P−Pd−P angle, thus copying the "chain effect".[19] What is the role of this angle?

To understand the impact of the P−Pd−P angle on the stability of palladium complexes, we review first the Walsh diagram picture in Figure 9 for a PdL_2 complex.[10] It is seen that bending of the L−Pd−L angle causes two important effects, destabilization of the HOMO and stabilization of the LUMO of the complex, compared with the linear fragment. Thus, with small chelating diphosphine ligands and in the presence of Cl^-, the P−Pd−P angle is kept small throughout the oxidative addition process, and the HOMO−LUMO gap of the complex remains small.[14a,b] How does the HOMO−LUMO gap affect the oxidative addition barrier? This question can be answered by following Su et al.[14a] using the valence bond states correlation diagram (VBSCD) model originally developed by Shaik et al.[21]

The VBSCD is described in Figure 10. It shows that the barrier for the oxidative addition arises from the avoided crossing of two state curves. One state describes the reactant state and is labeled as φ_1, and the other

(21) (a) Shaik, S.; Shurki, A. *Angew. Chem., Int. Ed. Engl.* **1999**, *38*, 586−625; *Angew. Chem.* **1999**, *111*, 616−657. (b) Pross, A.; Shaik, S. *Acc. Chem. Res.* **1983**, *16*, 363. (c) Shaik, S.; Hiberty, P. C. *Rev. Compt. Quantum Chem.* **2004**, *20*, 1−100. (d) Shaik, S. S. *J. Am. Chem. Soc.* **1981**, *103*, 3692−3701.

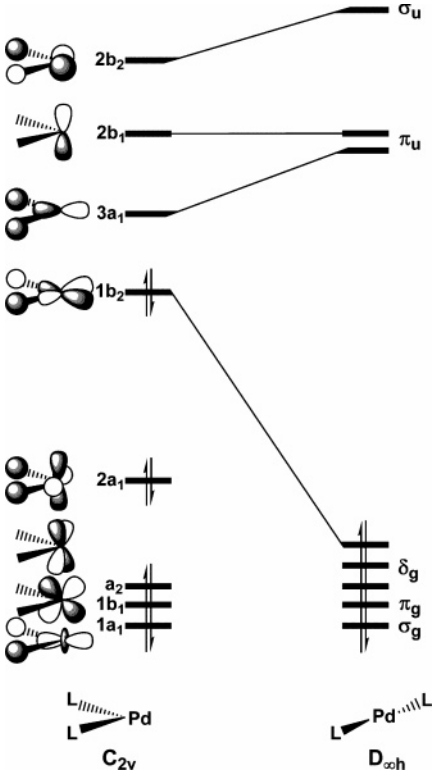

Figure 9. Walsh diagram for a PdL_2 fragment.

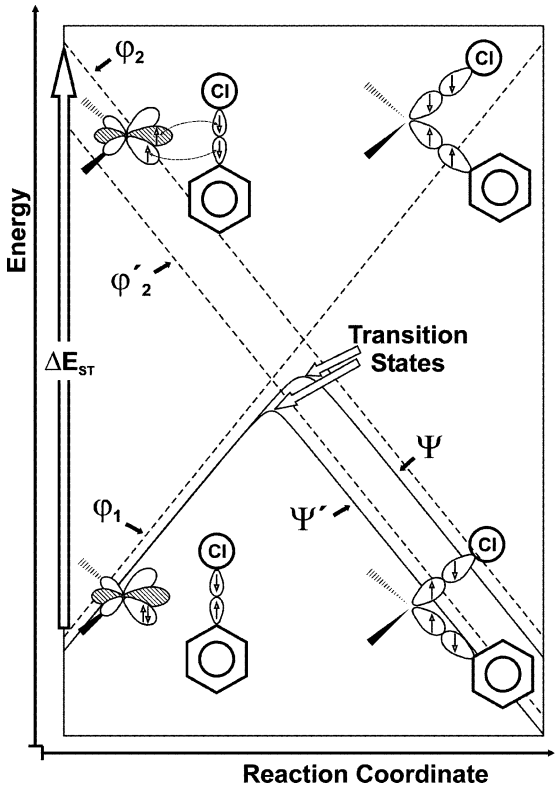

Figure 10. VBSCD diagram showing the origins of the barrier for the oxidative addition of Ph-Cl to a Pd catalyst. φ_1 and φ_2 are the reactant and product states. The Ψ values are the final states obtained from the mixing of the φ's. Lowering the singlet−triplet excitation by changing the catalyst to one having lower excitation energy (dashed line) lowers the respective transition state.

describes the product state and is labeled as φ_2. At the geometry of the reactants (left-hand side of the diagram), φ_2 is an excited state that involves singlet-to-triplet excitation of the paired electrons on the palladium catalyst and on the C−Cl bond; the resulting odd electrons are paired across the new linkages of the oxidative addition product, and the overall state is a singlet coupled.[21a] The excitation gap between the ground state φ_1 and the excited state φ_2, on the reactant side, is given by the sum of singlet−triplet excitations of the two reactants. In a series of reactions where the gap variable is dominant, the barrier along the series will decrease as the singlet−triplet excitation gap decreases. Su et al. have demonstrated amply the predictive ability of the model for a variety of oxidative addition processes.[14a]

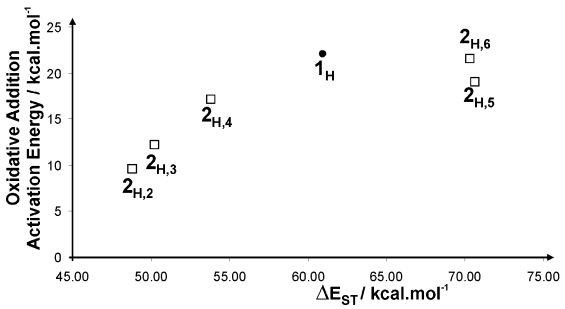

Figure 11. Dependence of oxidative addition activation energy on the singlet−triplet excitation of the Pd^0 catalyst.

For a fixed substrate as in our study, the only variable of the gap is the singlet−triplet excitation of the palladium catalyst, which involves excitation from the HOMO $1b_2$ to the LUMO $3a_1$ (see Figure 9 above) of the catalyst. Since a decrease in the P−Pd−P angle reduces the HOMO−LUMO gaps, it will decrease the corresponding singlet−triplet excitation and is expected therefore to reduce the oxidative addition barrier, as depicted pictorially in Figure 10.

A straightforward manifestation of this prediction is demonstrated in Figure 11, which plots the activation energies for the oxidative addition against the singlet−triplet excitation energies of the respective catalysts. The figure displays a general correlation of the barrier with the ΔE_{ST} quantity of the chelated catalysts, $\mathbf{2}_{H,n}$. As the methylene chain of the ligand gets longer, the P−Pd−P angle opens up (see Figure 4); the excitation energy of the catalyst increases and the oxidative addition barrier goes up. It is seen that the barriers for the largest ring, $n = 6$, is approximately equal to the barrier for the $Pd(PH_3)_2$ catalyst, $\mathbf{1}_H$. Placing the data point for $\mathbf{1}_{H,Cl}$ on this plot would require the anionic catalyst to have a small ΔE_{ST} quantity, as for the chelated catalyst $\mathbf{2}_{H,3}$, where the bite angle is 112.7° (Figure 3). How does the chloride anion additive maintain such a small ΔE_{ST} quantity?

We recall that, in the anionic catalyst, the Cl^- anion closes the P−Pd−P angle by coordination to Pd, and then it migrates in the transition state between the phosphine ligands, where it is stabilized by electrostatic interactions (Figures 5 and 6). Furthermore, the chloride anion clamps the phosphine ligands and decreases the P−Pd−P angle. Thus, in the case of $\mathbf{1}_{H,Cl}$ the P−Pd−P angle remains small throughout the oxidative addition process, thereby minimizing the singlet−triplet excitation. Following the above discussion, reduction of the singlet−triplet excitation leads to the calculated

small activation energy. In this sense, the anionic additive indeed copies the chelate effect.

B. Effect of the Additive on the Stability of the Nucleophilic Addition Product. As shown in Figure 8a, the chloride additive raises the energy of the nucleophilic addition intermediate, $\mathbf{II'}_{Cl}$, relative to the reactant state. As we have already reasoned above, *this effect is due to the displacement of the additive by the nucleophile*. Thus, in the cycle of the anionic catalyst, the initial stabilization exerted by the additive in the catalyst, $\mathbf{1}_{H,Cl}$, is lost as the additive is displaced by the nucleophile to yield the substitution product $\mathbf{II'}_{Cl}$. This, together with the lowering of the transition state for the oxidative addition, reduces the energy span of the cycle and thereby improves its turnover frequency (eq 3), compared with all other catalysts.

C. Overall Effect of the Additive on the Cycle. Especially illuminating is the comparison of the anionic catalyst with the chelated catalysts. Thus, chelating the palladium, with a small ring, has the benefit of reducing the barrier for oxidative addition, but the energy span of the respective cycle is not reduced, since the stabilization of the palladium complex by the small ring carries over to the substitution product. In contrast, the additive tunes the properties of the cycle by being present when needed (i.e. to reduce the barrier for oxidative addition) and absent when it is not necessary (i.e., in the substitution product). Thus, *under conditions of single turnover kinetics, the chelated catalysts can be as good or even better than the anionic catalyst, whereas under turnover conditions of a working cycle, the anionic catalyst will be preferable.*

The anionic additive exerts another beneficial effect on the catalytic cycle. Thus, as can be seen in Figure 8a, the catalyst−substrate cluster $\mathbf{C}_H$ is significantly more stable than the free reactants in the case of the anionic catalyst, whereas in the pristine catalyst the cluster is equienergetic with the free reactants (the same advantage will carry over to the free energy scale). As such, by analogy to an enzyme, the presence of Cl^- endows the palladium catalyst with a substrate binding mechanism, thereby preventing the diffusion away of the substrate and improving thereby the restart of the cycle.

D. Computed and Kinetically Based Cycles. Scheme 3 shows simplified representations of the kinetically based (in part a) and computed (in part b) catalytic cycles. The major difference is the presence of pentacoordinated complexes in the cycle in part a, and the absence of these in the computed cycle in part b. As noted above, pentacoordination was deemed implausible in several studies.[13b,16b] We must, however, recall that the tentative structure of the pentacoordinated complex $PhPdI(Cl)(PPh_3)_2^-$ was inferred from (i) the fact that the four-coordinate complex *trans*-$PhPdI(PPh_3)_2$ gives a *reduction peak only*, whereas the inferred new intermediate gave *an oxidation peak* (+0.40 V vs SCE at 0.2 V s^{-1}) after the oxidative addition of Ph−I to $Pd^0(PPh_3)_2Cl^-$, (ii) the depletion of the oxidation peak in time with the simultaneous appearance of *trans*-$PhPdI(PPh_3)_2$ and 1 equiv of chloride anion, and (iii) its ^{31}P NMR singlet.[5] As already mentioned, at the time, the intuitive and most reasonable interpretation of these findings was the pentacoordinate complex shown here

Scheme 3. Comparison of the Detailed Kinetically Derived Cycle (a) with the Computed Cycle (b) for an Anionic Catalyst

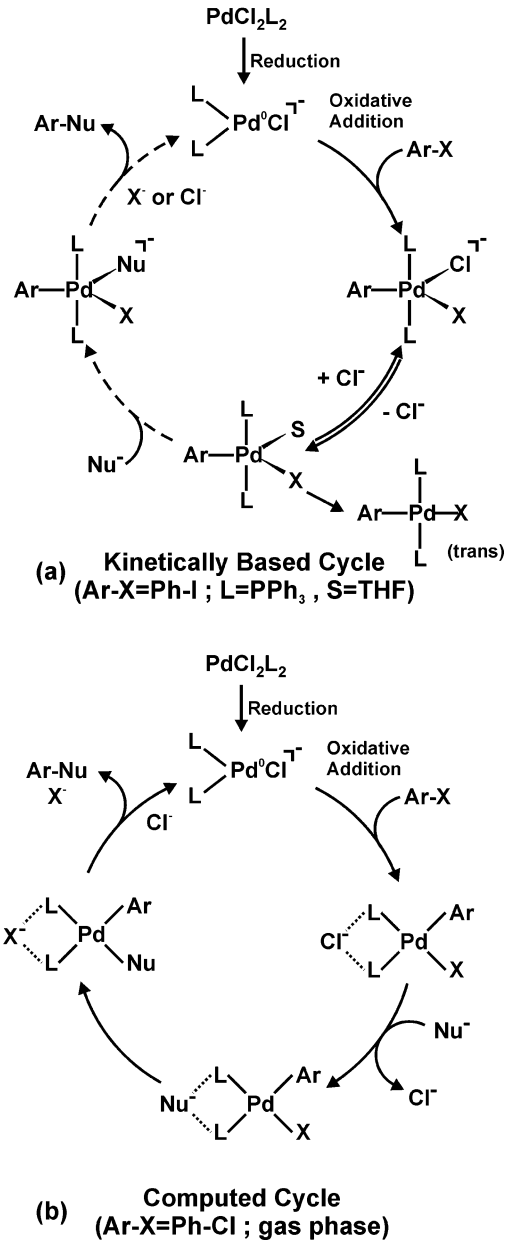

in Scheme 3a. However, on the basis of the computational studies here and elsewhere,[13b] we can propose that the initially postulated[5] pentacoordinate complex is the square-planar Pd(II) complex with the Cl^- electrostatically (some charge transfer is also apparent in Figure 6) coordinated to the phosphine ligands to create a semblance of pentacoordination. Other than this structural aspect, the computational study validates the kinetically derived cycle and projects the utmost importance of the anionic additive.

Conclusion

The efficiency of a catalytic cycle (Figure 1)[15] under turnover conditions is determined by the energy span quantity, δE, which measures the energy difference between the summit and deepest species of the cycle; the smaller the energy span, the higher the turnover

frequency of the cycle (eq 3). In this sense, the best Pd(0) catalyst for the cross-coupling reaction is that formed from the pristine species, Pd^0L_2 (L = phosphine in Scheme 3), by complexation of a chloride ion additive to form $Pd^0L_2Cl^-$. The DFT calculations and theoretical analysis show that the anionic catalyst thus formed is superior to the pristine species Pd^0L_2, since it flattens the energy landscape of the catalytic cycle, by stabilizing the transition state for oxidative addition, the summit of the cycle, and at the same time destabilizing the nucleophilic addition product, the deepest point of the cycle. This is precisely the role deduced initially from experimental evidence by two of us.[6,7]

The chloride additive achieves this effect in an intriguing manner. During substrate activation the Cl^- ion migrates to the back of the complex and clumps the phosphine ligands to keep a small P−Pd−P angle, which is a prerequisite for a low activation barrier to oxidative addition.[14a−c] In this respect, the chloride ion additive copies the effect of a bidentate phosphine ligand that maintains a small P−Pd−P angle by chelating the palladium. During nucleophilic substitution, the Cl^- additive is displaced by the nucleophile, and hence the stabilizing advantage is lost, thereby raising the substitution product complex relative to the onset of the reactants (Scheme 3, Figure 8a). After product release, Cl^- returns to complex the Pd^0L_2 species. The regenerated anionic catalyst $Pd^0L_2Cl^-$ then binds the substrate and prevents its diffusive escape, thereby ensuring an efficient restart of the cycle.

The computed energy advantage of the δE quantity, ca. 16 kcal/mol, and the complexation energies of Cl^-, in the range of 8−12 kcal/mol, correspond to gas-phase values. These values predict catalysis by many orders of magnitude (more than 10). However, these large values will certainly be attenuated in the presence of a solvent. Therefore, the question is: will the catalytic effects thus calculated persist? Answering this question will have to await an appropriate study of the entire catalytic cycle in THF as a solvent (using combined discrete plus continuum solvation) and a substrate more reactive than Ph−Cl. However, the facts that (a) the anionic complex $\mathbf{1}_{H,Cl}$ was found to persist[10] also in solvent models, (b) the interactions of Cl^- with the phosphine ligands in the oxidative addition transition state are of the same magnitude as in $\mathbf{1}_{H,Cl}$ and $\mathbf{1}_{Ph,Cl}$ and are competitive with the interaction with THF molecules, and (c) $\mathbf{TS}_{H,Cl}{}^{ox}$ remained intact after optimization in the presence of a $(THF)_7$ cluster all suggest that the effect discussed in this study may carry over, albeit in an attenuated form, to the situation in a solvent such as THF. Furthermore, the solvent and other additives may well play a role in the mechanistic steps of the cycle, e.g., by assisting the displacement of the additive by the nucleophile, which is essential for keeping a low energy span.

Acknowledgment. The research was supported in part by a common grant to the two groups from the Israeli Ministry of Science and the AFISRT in France (No. 991 MAE CCF5), and in part by a BMBF-DIP grant to S.S. (No. DIP-G.7.1) and from the CNRS, ENS and Research Ministry (No. UMR 8640) to C.A. and A.J.

Supporting Information Available: Figures giving *xyz* structures and tables of energy values. This material is available free of charge via the Internet at http://pubs.acs.org.

OM050160P